Distribution Category:
LMFBR Fuels and Materials
Engineering and Development
(UC-79b)

ANL-78-84

ARGONNE NATIONAL LABORATORY
9700 South Cass Avenue
Argonne, Illinois 60439

AN ULTRASONIC SCANNER FOR STAINLESS STEEL WELD INSPECTIONS

by

D. S. Kupperman and K. J. Reimann

Materials Science Division

September 1978

TABLE OF CONTENTS

	Page
ABSTRACT	7
I. INTRODUCTION	7
II. EXPERIMENTAL APPARATUS	8
III. DATA ACQUISITION	15
IV. SPECIMENS USED IN INITIAL TESTS	18
V. RESULTS AND DISCUSSION	20
VI. SUMMARY	31
VII. ACKNOWLEDGMENTS	31
REFERENCES	33

LIST OF FIGURES

No.	Title	Page
1.	Schematic Representation of Weld Scanner	9
2.	Acoustic Path for Scanner	11
3.	Detailed Photographs of Weld Scanner	12
4.	Schematic Representation of Electronic Apparatus for Weld Scanner.	14
5.	Block Diagram for Computer and Transient Recorder	16
6.	Flow Chart for Summing Digitized Wave Forms	16
7.	Flow Chart for Transferring Data on One Waveform to Nova 2	16
8.	Samples Employed in the Present Study	19
9.	Wall-thickness Measurement of Cast Stainless Steel Specimen Using Signal-averaging Technique	21
10.	Comparison of Single Digitized Waveform and Average of Eight Traces	23
11.	Schematic of Weld Scanner Showing Acoustic Path for the Detection of a Sample Edge	23
12.	Digitized Wave Form of Single Echo from Sample of Fig. 11	24
13.	Average of Nine Digitized Wave Forms from Scan of Sample in Fig. 11	24
14.	Sample and Transducer Arrangement for Signal Averaging to Enhance Signal to Spatial Noise Ratio for Crack Detection	26
15.	Five Oscilloscope Traces and Computer Average of Ten Traces for System Shown in Fig. 14, with Beam Reflecting off Crack Plane	26
16.	Five Oscilloscope Traces and Computer Average for System Shown in Fig. 14, with Beam not Reflecting off Crack Plane	27
17.	Five Oscilloscope Traces and Computer Averaged Output Showing Enhanced Signal-to-Noise Ratio for Notch Detection in Weld Sample Number 2 of Figure 8	27

LIST OF FIGURES

No.	Title	Page
18.	Arrangement of Scanner and Specimen for Detection of Weld-metal Notch	29
19.	Three Individual Traces and Computer Average of 10 Traces from Improved Notch-detection System Shown in Fig. 18	29
20.	Three Individual Traces and Computer Average of 10 Traces from System Shown in Fig. 18	30
21.	Three Individual Radio-frequency A-scan Printouts and Computer Average of 10 Scans	30
22.	Arrangement of Scanner and Cracked Welded SS Tensile Specimen for Detection of Weld-metal Crack	30
23.	Three A-scan Traces and 10-trace Average for Crack Detection in Sample Shown in Fig. 22	32

AN ULTRASONIC SCANNER FOR STAINLESS STEEL WELD INSPECTIONS

by

D.S. Kupperman and K.J. Reimann

ABSTRACT

The large grain size and anisotropic nature of stainless steel weld metal make conventional ultrasonic testing very difficult. This paper evaluates a technique for minimizing the coherent ultrasonic noise in stainless steel weld metal. The method involves digitizing conventional "A-scan" traces and averaging them with a minicomputer. Results are presented for an ultrasonic scanner which interrogates a small volume of the weld metal while averaging the coherent ultrasonic noise.

I. INTRODUCTION

Unlike ferritic steels, austenitic stainless steel (SS) does not undergo a phase transformation during cooling. Thus, slow cooling of SS weld metal leads to the formation of large, columnar grains which are not present in ordinary steel. The grains have a dendritic structure and tend to grow with a <100> orientation.[1] In a typical V-type weld, they grow perpendicular to the sides of the base-metal "V" for a distance of a few millimeters and then move upward in the weld metal, following the lines of heat dissipation.

Because of the large grain size and anisotropic nature of the weld metal, ultrasonic inspection of austenitic SS welds is extremely difficult. The ultrasonic attenuation in the weld material is much greater than that observed in the base metal. Spurious ultrasonic signals from the dendritic weld structure and beam steering can lead to difficulties in data interpretation. Thus, adequate flaw identification and characterization are inhibited.

The difficulties encountered in ultrasonic examination of SS are described in several recent papers and reports.[1-5] The problem in inspecting austenitic SS weld metal often reduces to one of extracting the flaw signal from the noise signals. This problem is not necessarily related to the presence of electronic noise but to coherent noise; that is, grain-boundary scattering or scattering from rough surfaces or weld-metal interfaces. Kennedy and Woodmansee[6] discuss signal processing for ultrasonic inspections. They have examined signal-averaging and cross-correlation techniques with multiple transducer arrays to improve signal to coherent noise ratios. Examples are presented in their paper demonstrating (a) the effect of signal averaging on crack detection in an electron-beam weld, and (b) detection of artificial reflectors in a titanium plate by cross-correlation of signals from a multitransducer array. In their array, five transducers were directed toward the same volume in the sample. A definite improvement in signal-to-noise ratio was observed by this technique.

The present report describes a device that utilizes signal-averaging techniques for scanning an SS weld.

II. EXPERIMENTAL APPARATUS

A. Operation of the Weld Scanner

The weld scanner, shown schematically in Fig. 1, can be operated manually or adapted to automatic scanning. The base is about 20 x 12 cm and the maximum height is 20 cm. Water is used as a couplant. Two transducers (T and R in Fig. 1) are operated in a pitch-catch mode to generate 45° ultrasonic waves in SS samples. The projection of the pitch-catch included angle (θ) to a horizontal plane is varied between 60 and 90° in steps of $\sim$ 3°, and the receiving signal is averaged over several transducer positions. With each

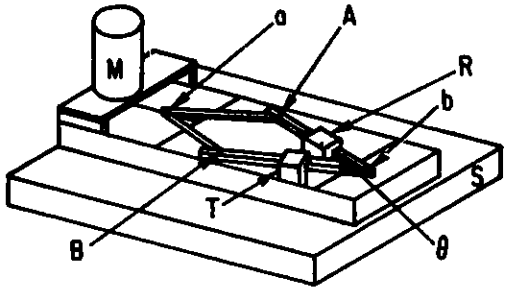

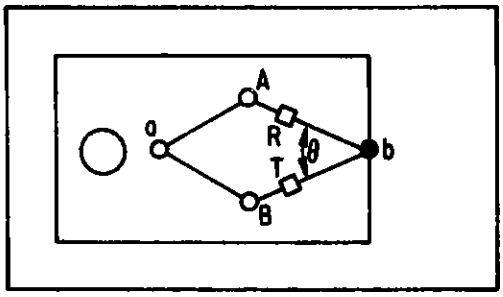

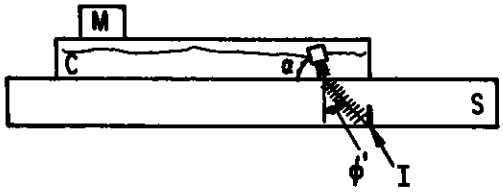

Fig. 1. Schematic Representation of Weld Scanner. M = motor, C = couplant, S = sample, I = point of intersection of ultrasonic beams, α = incident angle in water, θ = scan angle, b = fixed pivot point, R = receiving transducer, T = transmitting transducer, and ϕ' = angle of refraction in the sample. Neg. No. MSD 65552.

change in θ, the coherent scattering varies. If the intersection of the beam paths from the two transducers lies on a flaw, variation of the included angle may allow the flaw signal to remain strong while the noise signal varies. Even if the flaw signal is not present in all scan angles, origin of the flaw signal may be evident at several different angles. Thus, through signal averaging of different approach angles, the flaw becomes more apparent than if just one approach angle were used.

In practice, θ is varied as follows (with reference to Fig. 1): Point b is a pivot. Point a can move toward or away from b, and the transducers can move along arms A and B. Point I is the intersection point of the transmitting and receiving beams. ϕ' is varied by changing the angle α and then adjusting T and R along rods A and B so that I remains directly below b, while the vertical distance between I and b varies. When these adjustments are made properly, the total acoustic path-length remains constant. This is demonstrated geometrically in Fig. 2. The total acoustic path-length, L, consists of the path in the couplant from transducer to couplant-metal interface ($\overline{TO}$) plus the path in the sample ($\overline{OI}$). L is given by $h/\cos\phi + t/\cos\phi'$, where h is the vertical distance between transducer and sample; ϕ is the angle of incidence of the acoustic beam with the surface of the sample; t is the sample thickness; and ϕ' is the refracted beam angle. The values of h, ϕ, t and ϕ' all remain fixed as the 1/2-angle separating the arms of the scanner varies from 30 to 45°. Thus, L will be constant for all values of θ if the velocity of sound in the sample is uniform. In stainless steel weld metal, which is anisotropic, this velocity varies with θ. This causes some problems, which will be discussed in later sections.

Figure 3 shows more detailed views of the scanner. Two Aerotech, 1/4-in., 2.25-MHz gamma-series transducers were used. The angle θ was varied by using a cam-driven rod and Geneva mechanism. With this system, the dead

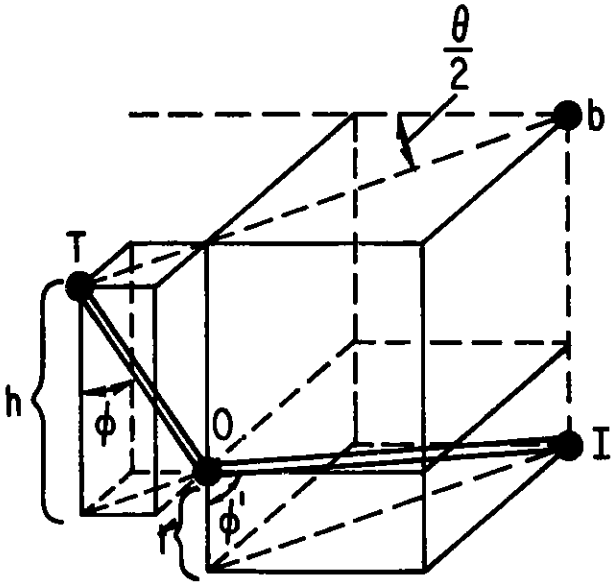

$$L = \frac{h}{\cos \phi} + \frac{t}{\cos \phi'}$$

Fig. 2. Acoustic Path for Scanner.
Neg. No. MSD 65550.

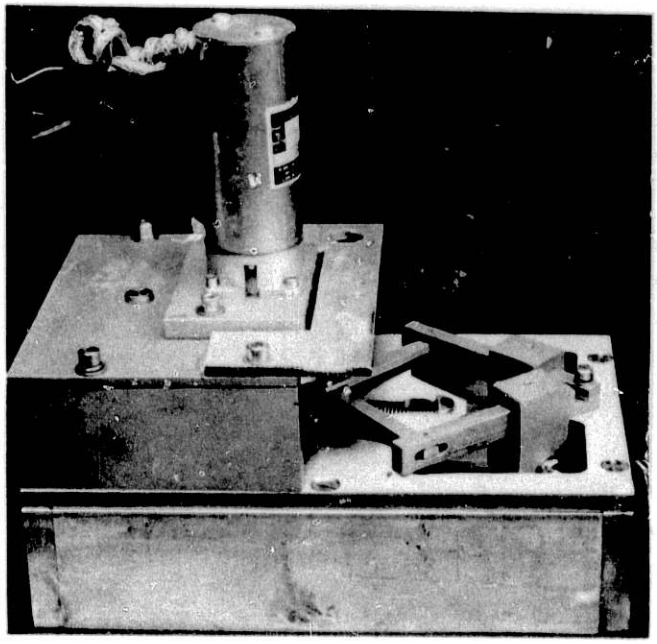

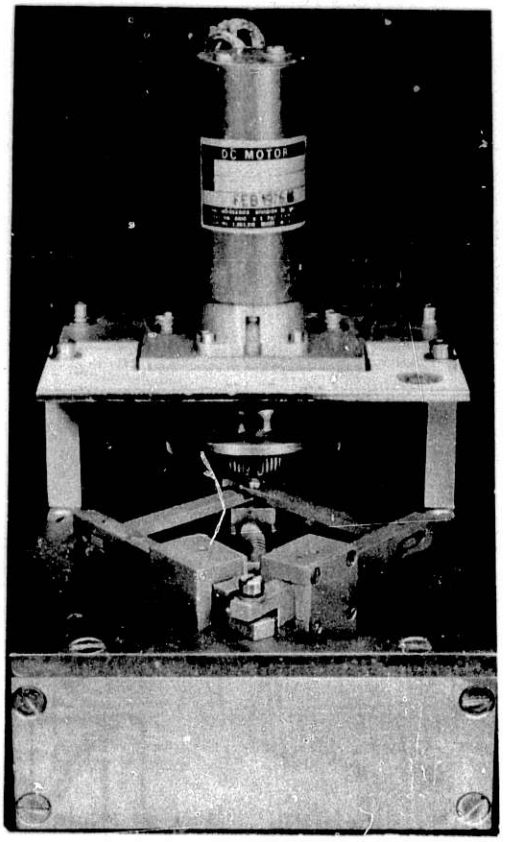

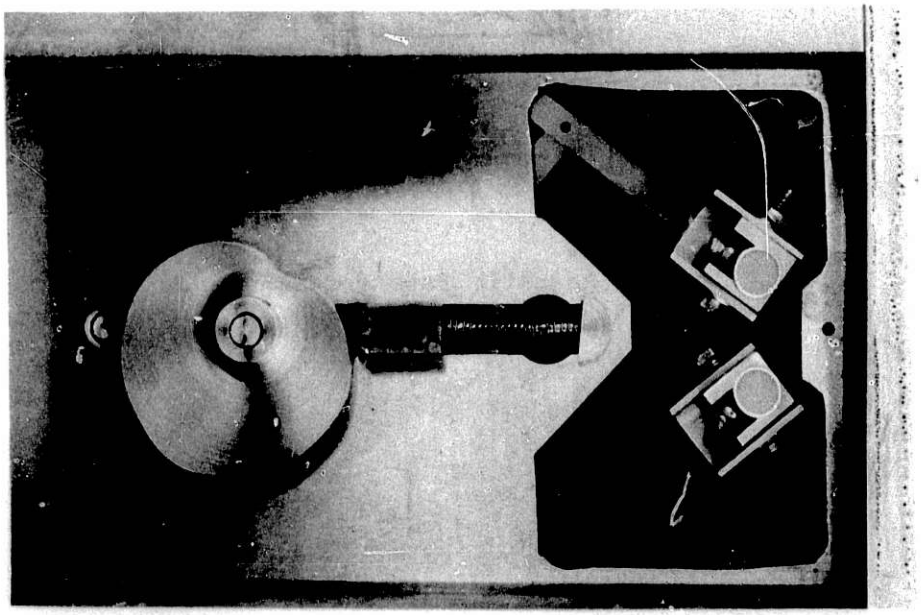

Fig. 3. Detailed Photographs of Weld Scanner. Neg. No. MSD 65516.

time (pause) between changes in the angle can be controlled by the motor speed which is determined by the DC voltage applied to it (30-V max). The scanner system can be operated using either mode-converted shear or refracted longitudinal beams.

B. Data Processing

During each pause, the ultrasonic trace or "A-scan" is digitized by a Biomation 8100 transient recorder and then stored in the memory of a Data General Corporation 2/10 Minicomputer. The average of digitized traces from up to 10 angular positions of the beams is printed out after the scan for a particular point in the sample is completed. As a result, one obtains a series of averaged A-scans as the weld scanner moves across the specimen.

Figure 4 shows a schematic representation of the electronic equipment used for this system. An Aerotech UTA pulser receiver for radio-frequency signals and a Sonic Mark I ultrasonic tester for video A-scans were used. The A-scan is digitized by a Biomation 610B or 8100 transient recorder which is triggered simultaneously with the "main impulse" of the pulser. The smallest sample time interval possible with the Biomation 8100 is 0.01 μs (0.1 with the 610B). Thus, with the 2048 memory channels in the 8100, 20 μs of data can be recorded at a 0.01-μs sampling time. This 20-μs "window" can be delayed from the main impulse by up to 10 μs (for a sampling rate of 100 MHz). At a 0.1-μsec sampling time the window is 200 μs and the delay 100 μs. The 2048 points in the Biomation 8100 are transmitted in 1 ms regardless of the rate at which they were acquired. Thus, for example, at a 0.01-μs sampling time, 20 μs of "real" time is represented on the oscilloscope by 1000 μs. For the 610B, there are 250 memory channels. The resolution for the vertical amplitude is 0.4% for the 8100 and 1.5% for the 610B. The

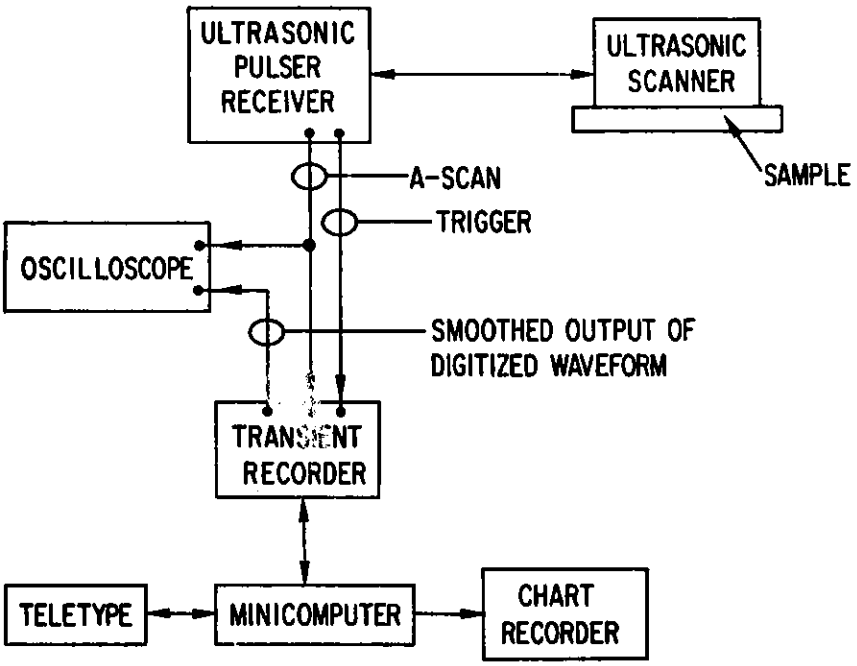

Fig. 4. Schematic Representation of Electronic Apparatus for Weld Scanner. Neg. No. MSD 65553.

digitized waveforms are stored and averaged in the Nova 2 minicomputer. The averaged A-scan is then plotted out on the x-y chart recorder.

A block diagram for the computer and transient recorder is shown in Fig. 5. The Nova 2/10 has a 32K word memory (16-bit word) and is interfaced to the Biomation 8100 (or 610B) with a Data General 4040 general-purpose interface board. The computer programs are developed on an IBM 370/195 which provides a binary tape output. The program is then read through the teletype and stored on magnetic tape.

The Biomation 8100 can be activated manually or automatically (from the scanner). After the waveform is stored in the Biomation transient recorder, it is transferred to the Nova 2/10 computer through program-data transfer. The computer accepts the digitized information channel by channel until it has recorded data from all channels. The second waveform is taken and data transferred to the Nova in the same way. This procedure is repeated to form the sum of up to 10 waveforms. By proper scaling of the x-y recorder, the average of the 10 waveforms is printed. Figure 6 shows a flow chart for summing the 10 waveforms and Fig. 7 the flow chart for taking the data of one waveform and transferring it to the computer.

III. DATA ACQUISITION

To operate the system with the UTA-3 pitch-catch mode (radio-frequency A-scans), the following procedure was used: From the model UTA-3, a gated signal was sent to one channel of the Biomation 8100 waveform digitizer. The signal was digitized and fed into a Tektronix 7904 oscilloscope. The oscilloscope trace allowed the individual digitized waveforms to be viewed and photographed. The Y output on the model 8100 was attached to the input of the model 7A26 dual-trace amplifier plug-in unit.

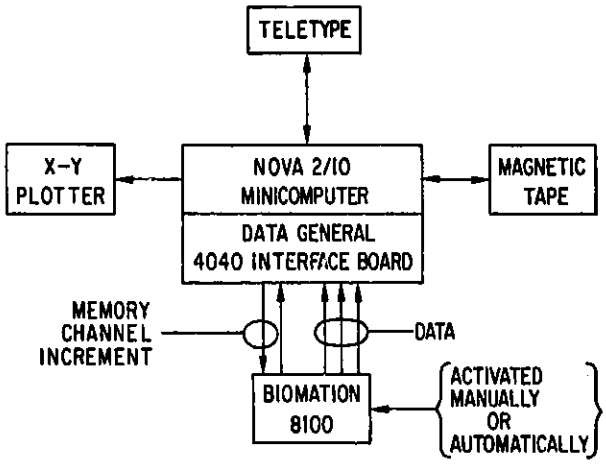

Fig. 5

Block Diagram for Computer and Transient Recorder. Neg. No. MSD 65554.

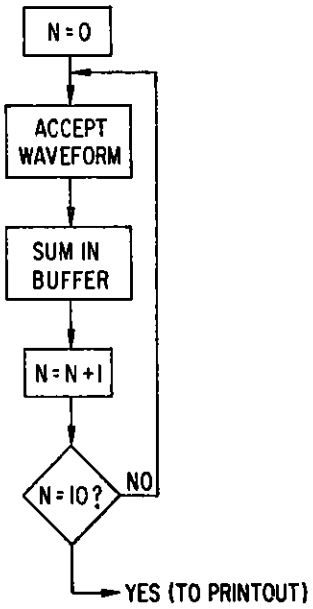

Fig. 6

Flow Chart for Summing Digitized Wave Forms. Neg. No. MSD 65555.

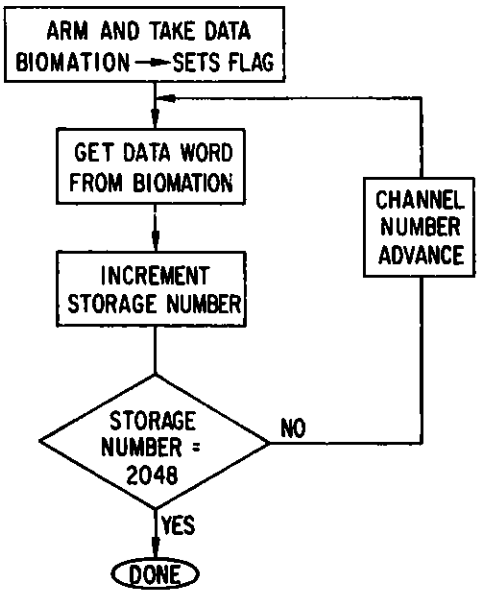

Fig. 7

Flow Chart for Transferring Data on One Waveform to Nova 2. Neg. No. MSD 65556.

When the Sonic Mark I was used, the transducers were hooked to the T and R inputs of the Mark I. Access output pins 4 and 6 were connected together and then wired to one of the Biomation 8100 channels and to a ground. The Y output of the model 8100 was hooked to the model 7A26-dual trace amplifier plug-in unit. The transient recorder was then interfaced to the computer.

After the electronics were set up and all the instrument-parameter adjustments were made, the software was loaded into the Nova 2/10. The computer responded with the following inquiries or orders:

SCANNER OR MANUAL?

This allowed the option of running the test either with the scanner with a ten-point average, or manually for checkouts or other purposes. The letter S was typed in, representing scanner. The computer then asked

BIOMATION 610B or 8100?

If the Biomation 8100 waveform digitizer was used during the experiments, the number 8 was the appropriate response; otherwise 6 was used. The computer replied with

DIGITAL AVERAGE PROGRAM:BIOMATION 8100

ARM AND TRIGGER.

to indicate that the system was armed and triggered.

After ten digitized waveforms had been sent to the computer, the computer stopped taking data. At this point, the computer responded with

SUM

TIME DOM

OUTPUT?(YES OR NO)

If the data were bad or if no output was desired, N, for NO, was the proper response.

If the output was desired, the letter Y, representing YES, was typed. The computer responded with

NUMBER OF POINTS = 002048

FIRST POINT =

The appropriate reply was between 0 and 2047, depending upon the part of the waveform to be viewed. The computer then asked

LAST POINT =

Here again, the response depended upon the part of the waveform desired. On receiving this response, the computer asked

TYPE OR DRAW?

The answer T, denoting TYPE, prompted the computer to type out the data on the teletype. When the answer was D, denoting DRAW, the computer asked

RANGE (POWER OF 2) (12 MAX)

The answer to this question determined the amplitude of the waveform to be drawn on the chart recorder.

IV. SPECIMENS USED IN INITIAL TESTS

Four SS samples, shown in Fig. 8, were used in the initial tests of this system. The first was a 30 x 5 x 1-cm 304 SS welded plate. The second was a 15 x 3.5 x 1-cm sample removed from the center of a 15 x 7.5 x 5-cm 304 SS welded plate. The area of the weld metal varied from 6.5 x 3.5 to 5 x 3.5 cm. At the center of this weld was a 0.4-mm-deep electric-discharge-machined (EDM) notch. The third sample, provided by Hanford Engineering Development Laboratory (HEDL), was a 1-cm-thick 304 SS welded tensile specimen with a fatigue crack $\sim$ 1 to 2 mm deep in the weld metal. The overall length of the specimen was 35 cm, and the width was 15 cm at the ends and 7.5 cm at the middle. The fourth sample was a welded piece of Fe-20Ni-20Cr stainless steel, $\sim$ 20 x 3 x 2.5 cm in size.

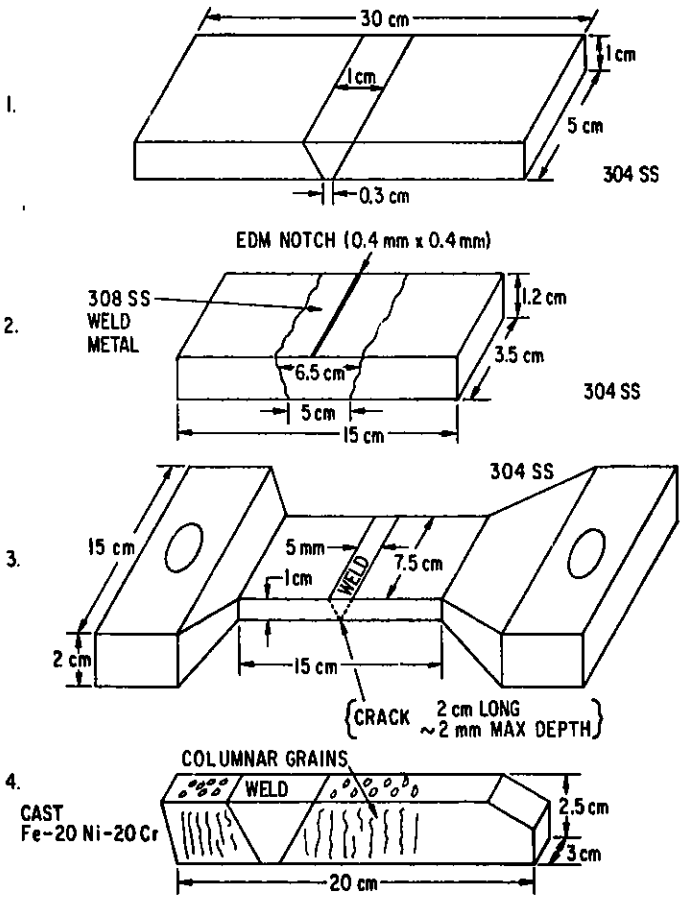

Fig. 8. Samples Employed in the Present Study.
Neg. No. MSD 65558.

V. RESULTS AND DISCUSSION

A. Demonstration of Concept

The concept of improving signal-to-noise ratios by averaging coherent noise can be readily demonstrated by an example where the thickness (25 mm) of a cast stainless steel specimen was measured. The sample used was number 4 in Fig. 8. An attempt was first made to measure the sample thickness, t, across the dendrites by conventional techniques. The A-scan in a pulse echo mode, using an Aerotech 2.25-MHz, longitudinal-mode contact transducer did not show a reflection off the back wall of the sample. The acoustic beam was traveling across the columnar grain structure; thus, the back wall echo was buried in the coherent noise caused by the grain-boundary scattering. If the transducer is moved slightly, the coherent noise pattern should change but the back wall echo should remain about the same. If many A-scan traces are averaged, the back wall echo should become larger in comparison to the noise. Figure 9 shows the results of this demonstration. The 6-mm-diameter transducer was moved within a 12-mm-diameter circle on one surface; the average of 20 radio-frequency "A-scans" is shown. The back-wall echo became clearly evident at 8 μs, whereas in the single traces no unambiguous back-wall echo was revealed. In this example, a transient-recorder sampling rate of 0.1 μs was used. The accuracy of the thickness measurement obtained by averaging 10 traces was ± 1%; averaging of more than 20 A-scans improved the accuracy very little. As a result of this test, it was decided that the feasibility of the signal-averaging concept could be demonstrated by averaging about 10 A-scan traces. Thus, the scanner was designed as previously described.

B. Triggering of Ultrasonic Signals

The accuracy of the spatial-averaging method depends critically on the ability to trigger each individual scan accurately enough so that the averaged

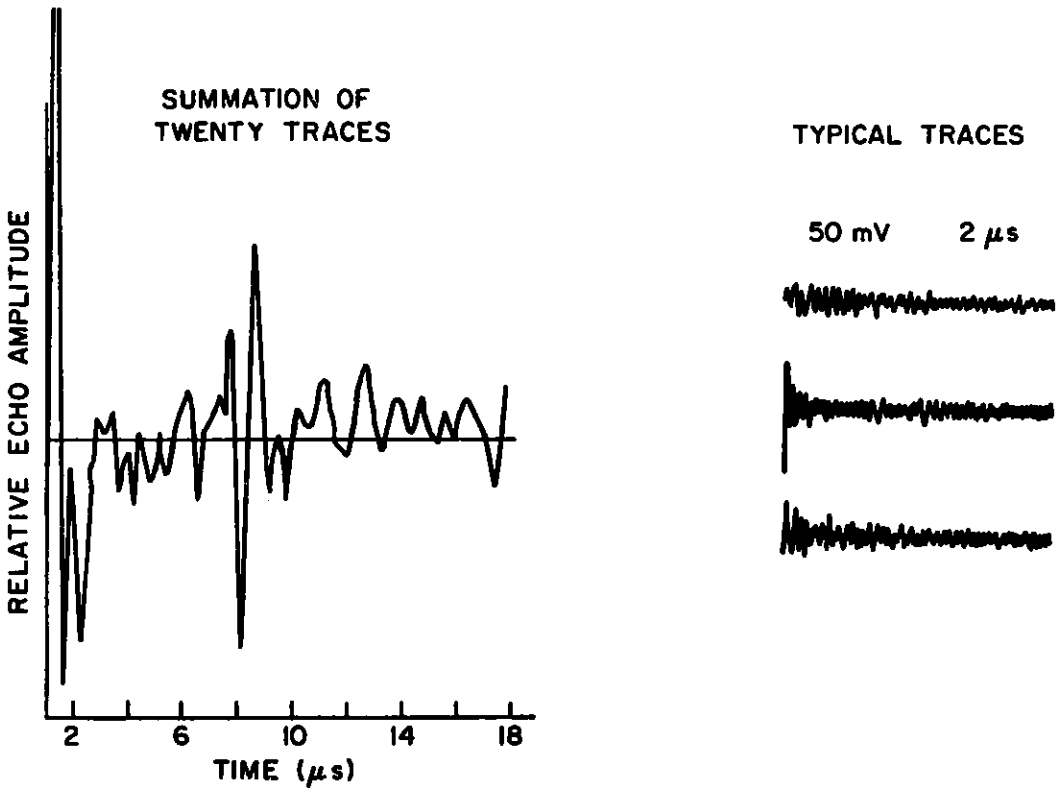

Fig. 9. Wall-thickness Measurement of Cast Stainless Steel Specimen Using Signal-averaging Technique. Neg. No. MSD 65560.

rf A-scans are all in phase and do not cancel each other out. The capability of the system to trigger properly is demonstrated in Fig. 10. The upper part of the figure shows a single digitized trace of a back-wall echo from a plexiglass block, made with a 2.25-MHz, 6-mm-diameter longitudinal mode transducer. The lower part of the figure shows the average of 8 separate traces. The eight traces were triggered manually and the sample time was 0.01 μs. Very little distortion of the waveform is evident. Figure 10 also shows a storage-oscilloscope trace which superimposes the eight rf traces. The ability of the system to reproduce a waveform accurately and to average without distortion is clearly demonstrated.

C. Detection of Edge of Weld-metal Sample

The ability of the scanner to improve signal-to-noise ratios was also demonstrated with a simple example. The objective in this case was to detect the edge of a specimen comprised partly of weld metal. Sample number 1 of Fig. 8 was used. A schematic of the scanner and sample are shown in Fig. 11. Also shown is the acoustic path for the detection of the edge of the Type 304 SS welded sample. Figure 12 shows the digitized rf signal of one echo from the sample edge, obtained from 2.25-MHz shear waves with probes operating in a pitch-catch mode. A sampling time of 0.1 μs was used. This sampling time results in a total range of 200 μs. Only a portion of the range printed out via a Nova 2 minicomputer is displayed here. In the single echo, the edge cannot be distinguished from the noise. However, by spatial averaging, we can extract the echo from the sample edge. Figure 13 shows the average of the digitized waveforms from nine angular positions of the weld scanner, for which the intersecting point of the transmitted and received ultrasonic beams remained fixed at the edge. The strongest peak is the sample edge.

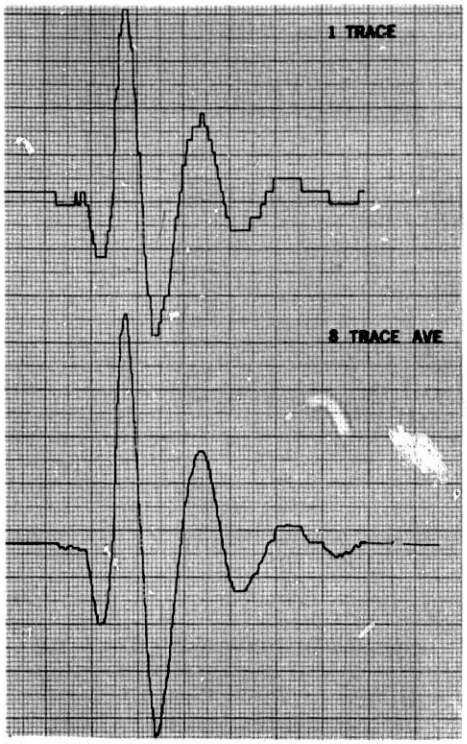

Fig. 10

Comparison of Single Digitized Waveform and Average of Eight Traces. The storage oscilloscope trace represents the superposition of eight traces. Neg. No. MSD 65562.

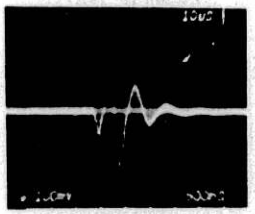

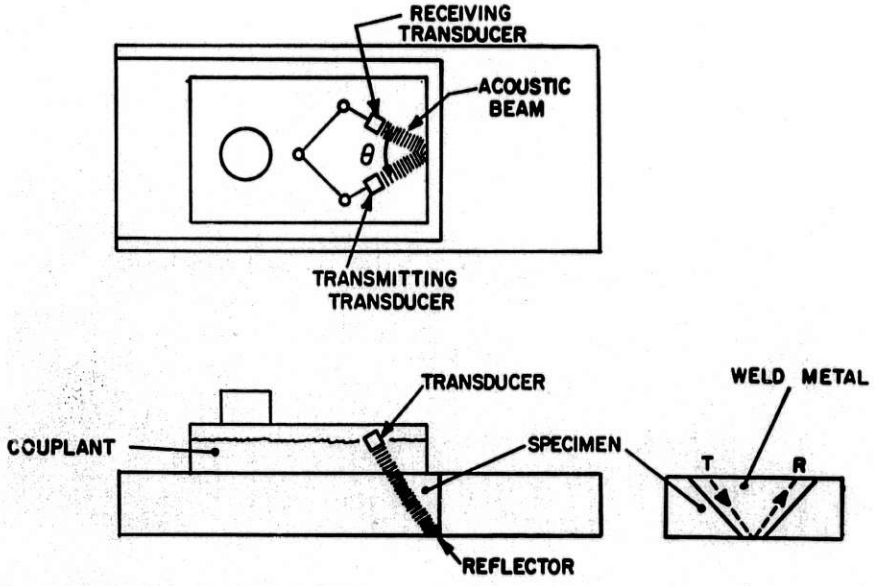

Fig. 11. Schematic of Weld Scanner Showing Acoustic Path for the Detection of a Sample Edge. Neg. No. MSD 65668.

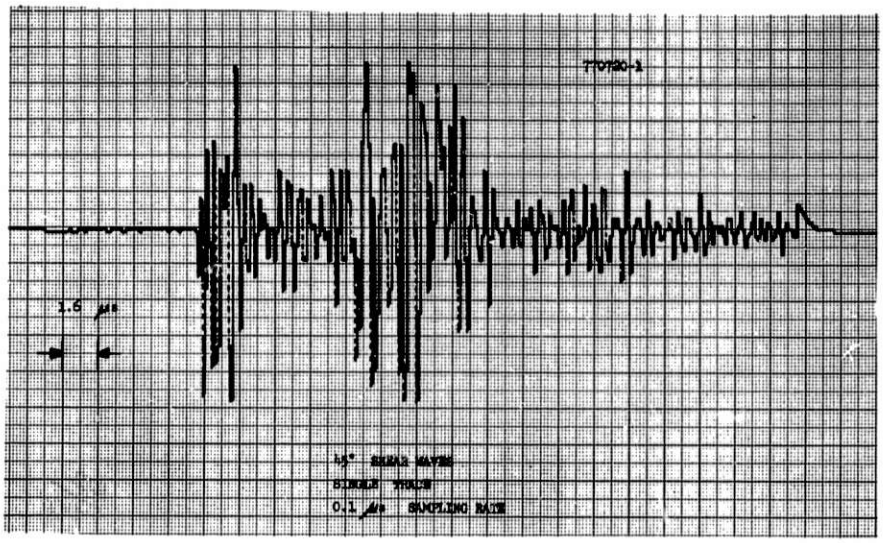

Fig. 12. Digitized Waveform of Single Echo from Sample of Fig. 11. Neg. No. MSD 65669.

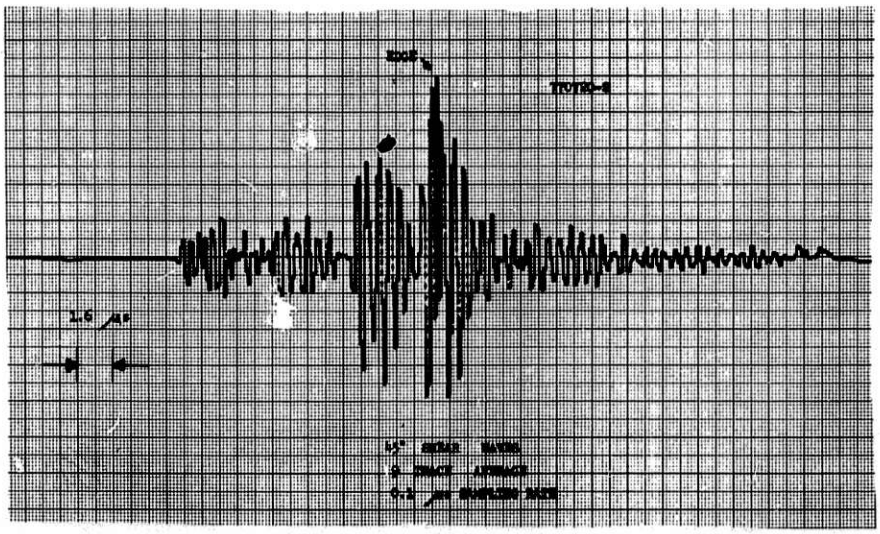

Fig. 13. Average of Nine Digitized Waveforms from Scan of Sample in Fig. 11. Neg. No. MSD 65670.

D. Detection of a Weld-metal Crack and Notch with a Single Probe

Another demonstration of the enhancement of signal-to-noise ratios was provided by the simplified system shown in Fig. 14. Here, an Aerotech miniature shear-wave transducer (6 mm, 2.25-MHz, 45° beam) was moved parallel to the plane of the crack (2 cm long and up to 2 mm deep) in sample number 3 of Fig. 8 (tensile specimen). Instead of the UTA-3, the Sonic Mark I with video output was used as the pulser-receiver. As will be seen, the smoothing of the rf traces can often enhance the ability to detect flaws with the signal-averaging process discussed in the present report. In this example, the transducer was displaced parallel to the crack plane in 3-mm steps. During this motion, 10 video traces, covering a total transducer displacement of 27 mm, were averaged to obtain the final A-scan. Figure 15 shows a typical averaged trace and five of the data sets in that average. The peak is the crack signal. The horizontal scale represents a time interval of 10 μs. The total acoustic path in the SS sample was 2.8 cm (transmission time 9 μs). For these traces, the A-scan was delayed by several microseconds with respect to the initial impulse. If the transducer is moved to a position ahead of the crack so that the beam still passes partially through the weld metal but does not impinge on the crack, the signal average should show a reduced noise level. Figure 16 shows an average of 10 traces with less background noise than in the individual traces.

The specimen (number 2 of Fig. 8) with an 0.4-mm-deep EDM notch in the weld metal was also tested with the system just described. The transducers were displaced in steps of 1.5 mm in a direction parallel to the notch. The average of 10 traces covers a 13.5-mm length of the notch. For this sample, the acoustic beam passed entirely through weld metal. An unambiguous notch signal is evident in the average trace shown in Fig. 17.

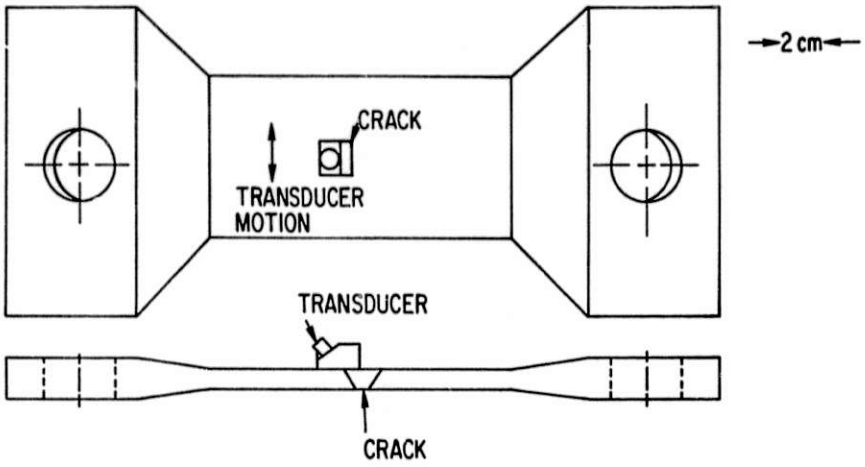

Fig. 14. Sample and Transducer (2.25-MHz, 45° Shear beam) Arrangement for Signal Averaging to Enhance Signal to Spatial Noise Ratio for Crack Detection. Neg. No. MSD 65557.

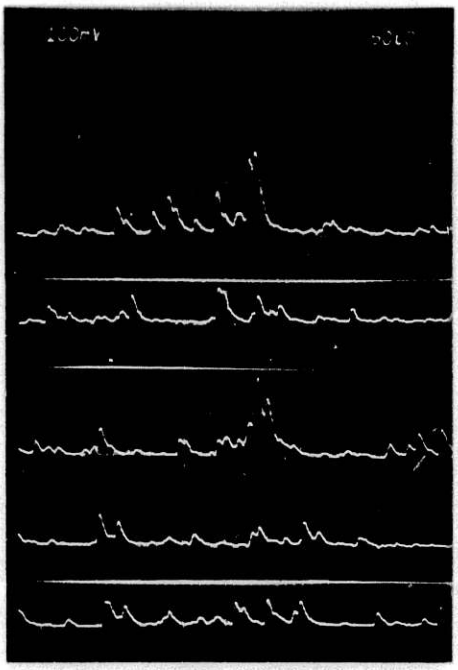

Fig. 15

Five Oscilloscope Traces and Computer Average of Ten Traces from System Shown in Fig. 14, with Beam Reflecting off Crack Plane. Neg. No. MSD 65565.

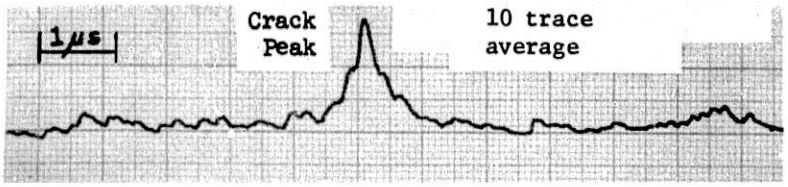

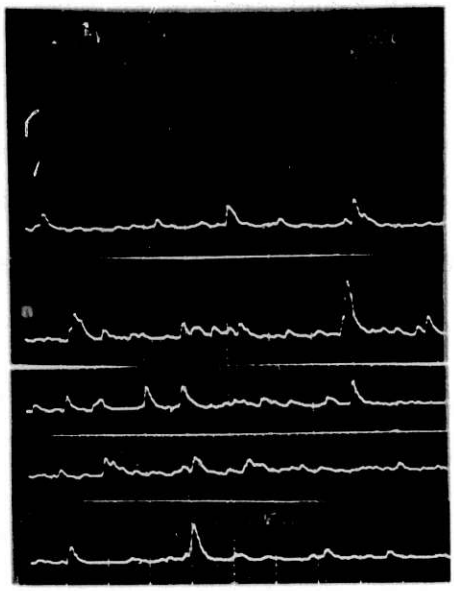

No Crack

10 trace
average

Fig. 16

Five Oscilloscope Traces and Computer Average for System Shown in Fig. 14, with Beam not Reflecting off Crack Plane. Neg. No. MSD 65564.

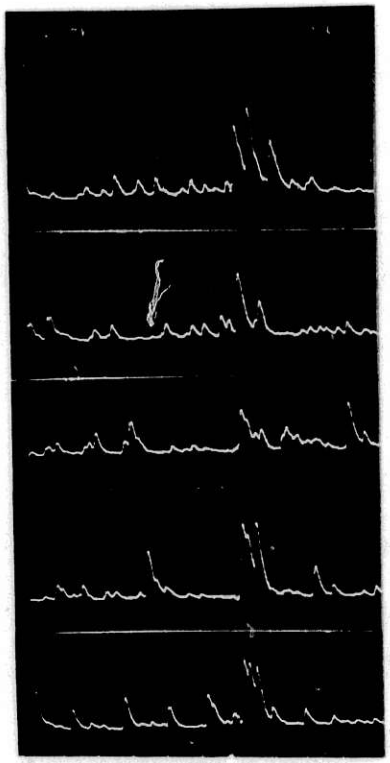

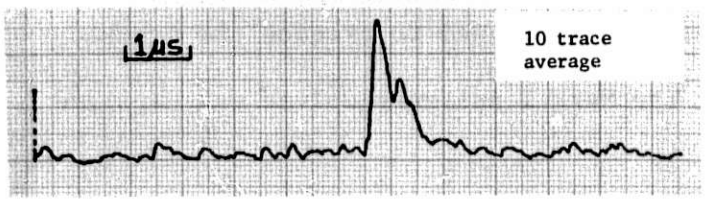

Fig. 17

Five Oscilloscope Traces and Computer-averaged Output Showing Enhanced Signal-to-Noise Ratio for Notch Detection in Weld Sample Number 2 of Fig. 8. A single 2.25-MHz, 45° shear-wave contact transducer was moved parallel to the notch in 1.5-mm steps to obtain these results. Neg. No. MSD 65561.

No spurious signals are visible as they were in the single A-scans. In general, the improvement in signal-to-noise ratio ranges from 6 to 20 dB.

E. Detection of a Weld-metal Notch with the Scanner

In this example, the weld scanner was used to examine the flat, wide weld in specimen number 2 of Fig. 8. The scanner orientation is shown in Fig. 18. Refracted longitudinal waves were used in this case (45°beam). Figure 19 shows the computer average of 10 A-scans (corresponding to 10 values of θ), and 3 individual traces. The transducer scanner was positioned so that ∿ 45° longitudinal waves were propagated in the weld metal. The averaged trace shows unambiguously the reflected longitudinal wave, the reflected shear and the shear-wave mode converted from a longitudinal wave in the EDM-notch plane. The trace average is about 20 μsec in length. The water-metal interface is seen as the first large peak. With the scanner away from the notch but still over weld metal, the averaged trace does not, as expected, show the presence of a reflector (Fig. 20). The acoustic beam was still traveling entirely in the weld metal. When the same specimen was examined with radio-frequency A-scans (still using 45° long waves), the results (Fig. 21) were not as good as with the video scan. The average of 10 traces, and the computer printout from 3 separate traces, are shown. Since the weld is anisotropic the velocity of sound in the weld metal depends on the propagation direction.[2] Thus, even though the pathlength was constant, the transit time varied slightly as the weld scanner changed the beam-propagation direction; consequently, the 10 traces are not in phase. With the video-scan output, this problem was eliminated.

F. Detection of a Weld-metal Crack with the Scanner

In the last example, the weld scanner was used to examine the cracked tensile specimen shown in Fig. 22. The Mark I pulser-receiver was employed

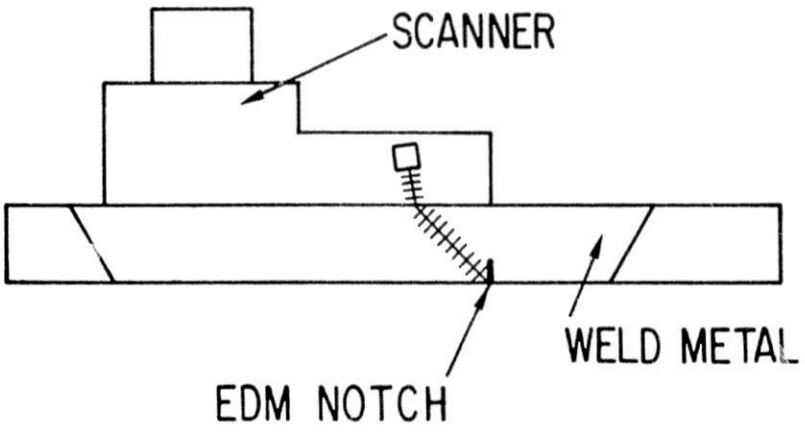

Fig. 18. Arrangement of Scanner and Specimen for Detection of Weld-metal Notch. The scanner generated 45° longitudinal waves in the weld metal. Neg. No. MSD 65551.

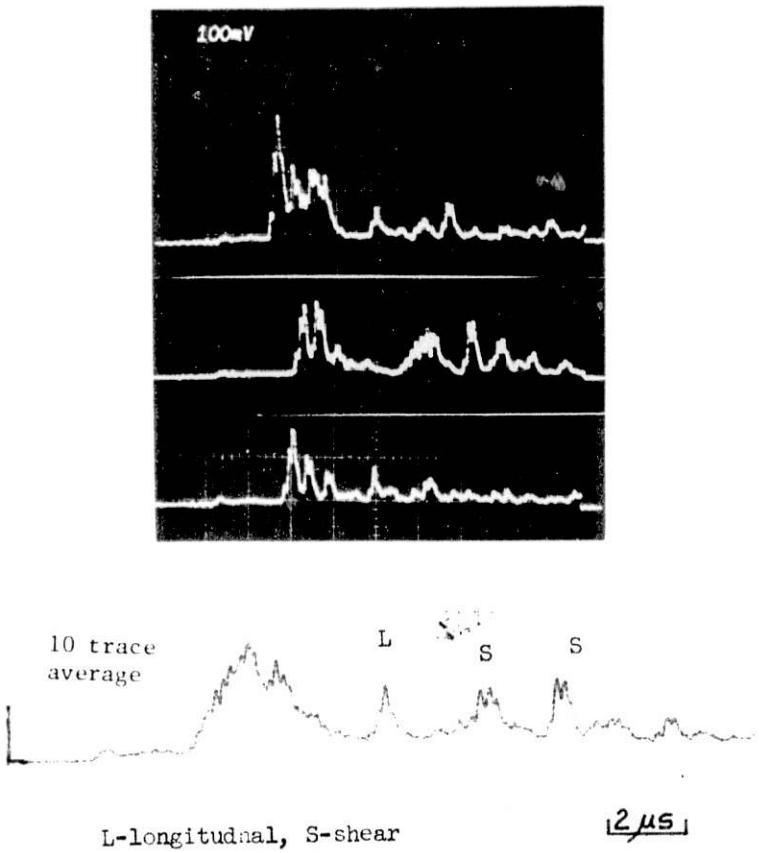

Fig. 19. Three Individual Traces and Computer Average of 10 Traces from Improved Notch-detection System Shown in Fig. 18. Refracted longitudinal and two shear waves can be seen. Neg. No. MSD 65566.

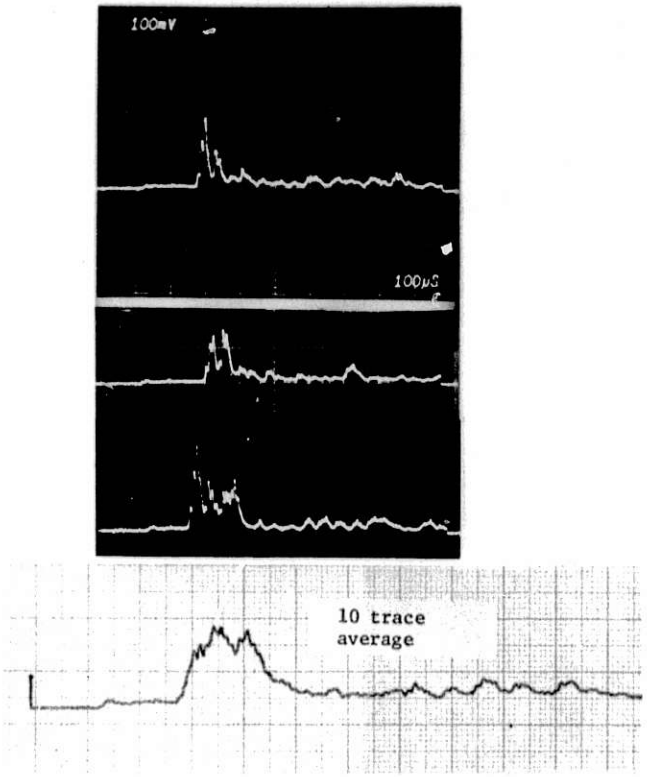

Fig. 20. Three Individual Traces and Computer Average of 10 Traces from System Shown in Fig. 18. While propagating in weld metal, the acoustic beam did not impinge on the notch plane. Reflections from the notch, seen in Fig. 19, are not evident here. Neg. No. MSD 65567.

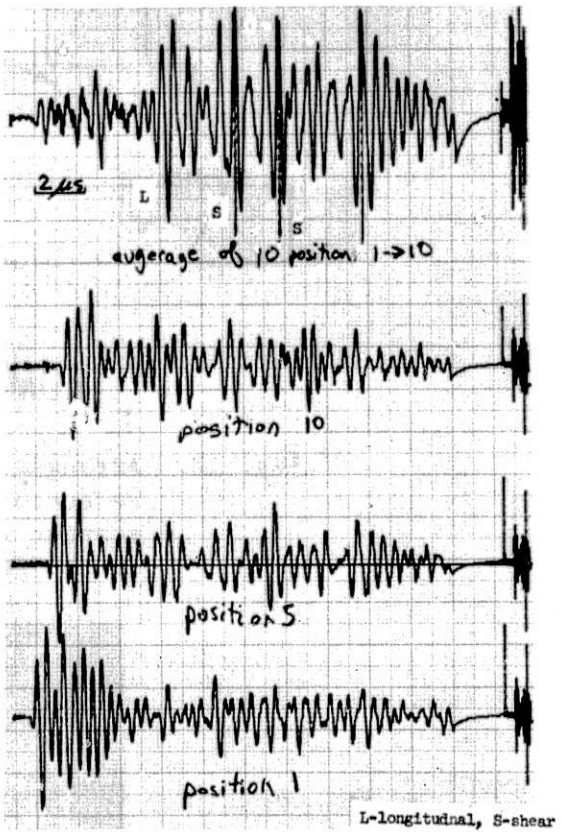

Fig. 21. Three Individual Radio-frequency (rf) A-scan Printouts and Computer Average of 10 Scans. Arrangement identical to that for Fig. 19, where A-scans were rectified and smoothed. Neg. No. MSD 65563.

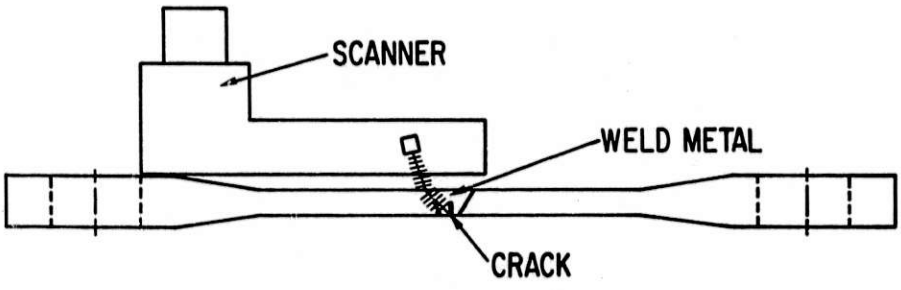

Fig. 22. Arrangement of Scanner and Cracked Welded SS Tensile Specimen (supplied by HEDL) for Detection of Weld-metal Crack. Neg. No. MSD 65559.

to take advantage of the video output. Figure 23 shows the result of a 10-scan average and 3 of the individual A-scans. An improvement in signal to coherent noise ratio is also seen in this example.

SUMMARY

The large grain size and anisotropic nature of stainless steel weld metal make conventional ultrasonic testing very difficult. Coherent ultrasonic noise from the weld metal masks signals from flaws. The present study demonstrates that the coherent ultrasonic noise can be averaged so as to significantly enhance the signal-to-noise ratio for flaws in stainless steel weld metal. This was accomplished with a device that varies the ultrasonic beam's angle of approach to a flaw so that the spatial noise varies while the flaw signal does not. An ultrasonic weld scanner has been demonstrated using weld samples containing both artificial and natural flaws. The weld scanner was designed and built to be interfaced with a transient recorder and minicomputer to carry out the signal-averaging procedure. The results of this effort have shown that coherent noise can be reduced by averaging, and the signal to coherent noise ratios improved by up to 20 dB over conventional ultrasonic techniques.

Acknowledgments

The authors wish to thank H.C. Russell for designing the scanning mechanism, A.L. Winiecki for assistance with the computer interfacing and software, W.D. Deininger for helping with data acquisition and analysis, Hanford Engineering Development Laboratory for lending us one of the specimens, and N.F. Fiore for supplying the cast stainless steel sample.

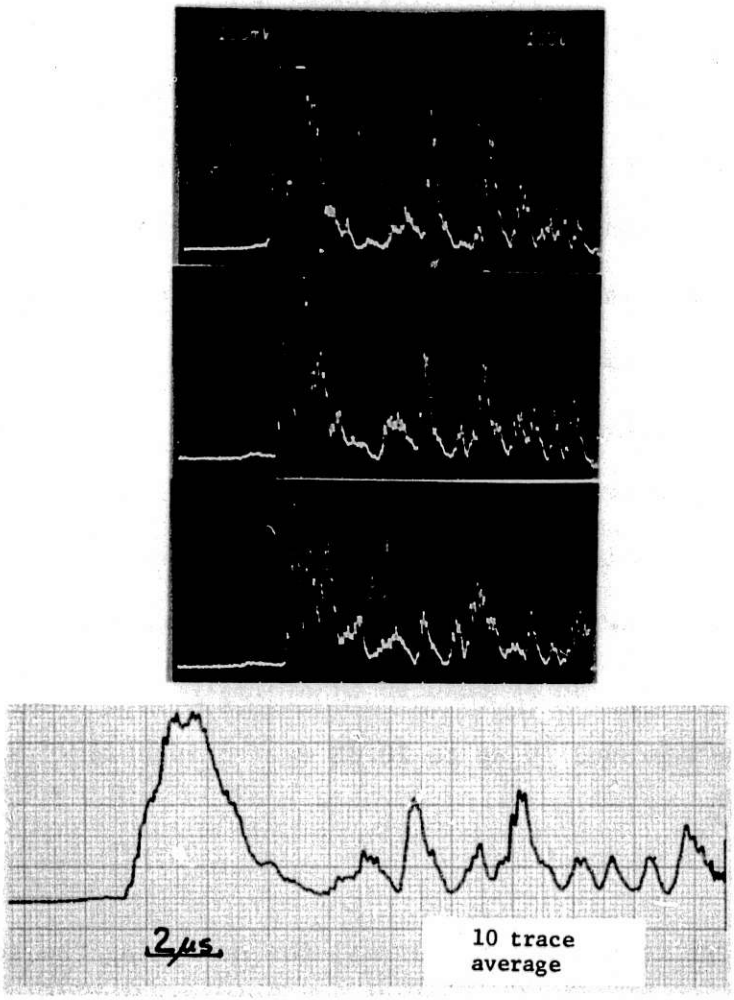

Fig. 23. Three A-scan Traces and 10-trace Average for Crack Detection in Sample Shown in Fig. 22. Neg. No. MSD 65568.

REFERENCES

1. D.S. Kupperman and K.J. Reimann, Ultrasonic Wave-propagation Characteristics and Polarization Effects in Stainless Steel Weld Metal, Argonne National Laboratory, ANL-78-29 (March 1978).

2. D.S. Kupperman, K.J. Reimann and N.F. Fiore, "Role of Microstructure in Ultrasonic Inspectability of Austenitic Stainless Steel Welds," Mater. Eval., 36 (5), 81 (1978).

3. J.J. Mech and T.E. Michaels, "Development of Ultrasonic Examination Methods for Austenitic Stainless Steel Weld Inspection," Mater. Eval. 35 (7), 81 (1977).

4. E. Neumann, M. Romer, T. Just, E. Nabel, K. Matthies, and E. Mundry, Development and Improvements of Ultrasonic Testing Techniques for Austenitic Nuclear Components, presented at Second Intl. Conf. on Non-Destructive Evaluation in the Nuclear Industry, Salt Lake City, Feb. 13-15, 1978.

5. B.L. Baikie, A.R. Wagg, M.J. Whittle, and D. Yapp, "Ultrasonic Inspection of Austenitic Welds," J. Brit. Nucl. Eng. Soc., 15 (3), 257 (1976).

6. J.C. Kennedy and W.E. Woodmansee, "Signal Processing in Nondestructive Testing," J. Test. Eval. 3 (1), 26-45 (Jan 1975).

Distribution for ANL-78-84

Internal:

J. A. Kyger
R. Avery
L. Burris
D. W. Cissel
S. A. Davis
B. R. T. Frost
D. C. Rardin
R. J. Teunis
C. E. Till
R. S. Zeno
H. O. Monson
R. W. Weeks
F. A. Nichols
L. T. Lloyd
J. F. Schumar
E. M. Stefanski (3)
T. H. Blewitt
M. B. Brodsky
W. J. Shack
F. Y. Fradin
A. G. Hins
A. P. L. Turner
K. L. Merkle
M. H. Mueller
R. B. Poeppel
R. W. Siegel
D. Stahl
H. R. Thresh
H. Wiedersich
T. F. Kassner
E. Fisher
D. S. Kupperman (10)
K. J. Reimann (10)
A. B. Krisciunas
ANL Contract Copy
ANL Libraries (5)
TIS Files (6)

External:

DOE-TIC, for distribution per UC-79b (259)
Manager, Chicago Operations Office
Chief, Office of Patent Counsel, CH
Director, Reactor Programs Div., CH
Director, CH-INEL
Director, DOE-RRT (2)
President, Argonne Universities Association
Materials Science Division Review Committee:
E. A. Aitken, General Electric Co., Sunnyvale
G. S. Ansell, Rensselaer Polytechnic Inst.
R. W. Balluffi, Massachusetts Inst. Technology
R. J. Birgeneau, Massachusetts Inst. Technology
S. L. Cooper, U. Wisconsin
C. Laird, U. Pennsylvania
M. T. Simnad, General Atomic
C. T. Tomizuka, U. Arizona
A. R. C. Westwood, Martin Marietta Labs.